The 2023 World Congress on
Advances in Structural Engineering and Mechanics (ASEM23)
GECE, Seoul, Korea, August 16-18, 2023

3D finite element modeling of externally prestressed concrete beams

Zhangxiang Li[1], Sensen Shi[2] and *Tiejiong Lou[3]

[1), 2), 3)] *School of Civil Engineering and Architecture, Wuhan University of Technology, Wuhan 430070, PR China*
[3)] *CEMMPRE, ARISE, University of Coimbra, Coimbra 3030-788, Portugal*
[3)] loutiejiong@dec.uc.pt

ABSTRACT

External prestressing has been widely applied in the construction and strengthening of structural engineering. This paper presents a 3D finite element model (FEM) developed in ABAQUS for nonlinear analysis of externally prestressed concrete beams. The validity of the finite element model (FEM) is verified by comparing the predicted load-deflection behavior with the test results of externally prestressed beam specimens available in the literature. Numerical assessments are then performed on simply supported externally prestressed concrete beams, with investigated variables including the type of rebars and the concrete grade. The results indicate that the beams with CFRP rebars exhibit better crack mode and higher ultimate load than the beams with GFRP or steel rebars, and also show that a higher concrete grade leads to a greater flexural capacity of the beams.

1. INTRODUCTION

In civil engineering, reinforced concrete structures are frequently used due to their high load-bearing capacity and excellent stability, but the issue of structural carbonation and corrosion of steel reinforcements caused by the complex environment has been of great concern [1]. External prestressing provides a variety of benefits, including increased structural capacity [2], improved cracking and better shear capacity [3], and simple replacement of external tendons. As a result, external prestressing is a promising technology to strengthen concrete structures [4]. The benefits of FRP materials, which primarily include CFRP, GFRP, BFRP, and AFRP, are their high strength and light weight, as well as their excellent fatigue resistance and corrosion resistance. Therefore, they have outstanding performance whether utilized as bonded rebars in concrete or external

---

[1)] Graduate Student
[2)] Graduate Student
[3)] Professor

tendons to support bridge construction. ACI 440.1R-15 [6] provides detailed instructions on the requirements for the arrangement of FRP rebars in concrete. Researchers have evaluated the static behavior of FRP-reinforced structures [7-9] and their dynamic fatigue behavior [10-11] for the past twenty years.

Numerical simulations are being widely utilized to examine the short- and long-term mechanical behavior of externally prestressed structures. By developing a detailed 3D FEM for three typical externally prestressed steel plate girders, Lin et al. [12] investigated the behavior of these structures and confirmed their dependability and stability by comparing the fracture safety factors. By utilizing the ABAQUS software, Tran et al. [13] developed a FEM for precast segmental concrete girders with external FRP tendons, taking into account the second-order effects caused by the change in tendon eccentricity. They discovered that replacing external steel tendons with high-modulus (E_P = 200 GPa) CFRP ones increased the stiffness and strength of precast segmental concrete girders while decreasing their ductility. Additionally, the analytical model currently in use to calculate the stress (f_{pu}) and effective depth (d_{pu}) of the external FRP tendons was assessed. The results indicated that the analytical model were not very conservative.

Based on the existing tests in the literature, a refined 3D FEM for externally prestressed concrete beams is developed by using AQAQUS in this study. The model is verified with experimental results. A numerical study is then performed to evaluate the behavior of externally prestressed concrete beams, focusing on the effect of the type of rebars and the concrete grade.

2. TEST OVERVIEW AND ESTABLISHMENT OF FEM

2.1 Information of test Program

Six simply supported T-beams with external tendons under third-point loading up to failure as reported by Tan et al [14] were selected and the mechanical behavior of the structure was investigated. The test was to investigate the impact of the position and number of deviators on the behaviors of the structure. Six 3.3 m T-beams were ready and Fig. 1 shows steel rebar characteristics and section specifications. Based on the material and geometric non-linearity of the model, three of the six beams (T-0, T-1, and T-2) were selected as typical beams (see Fig. 2), and the FEM results were compared with laboratory tests to validate the proposed model.

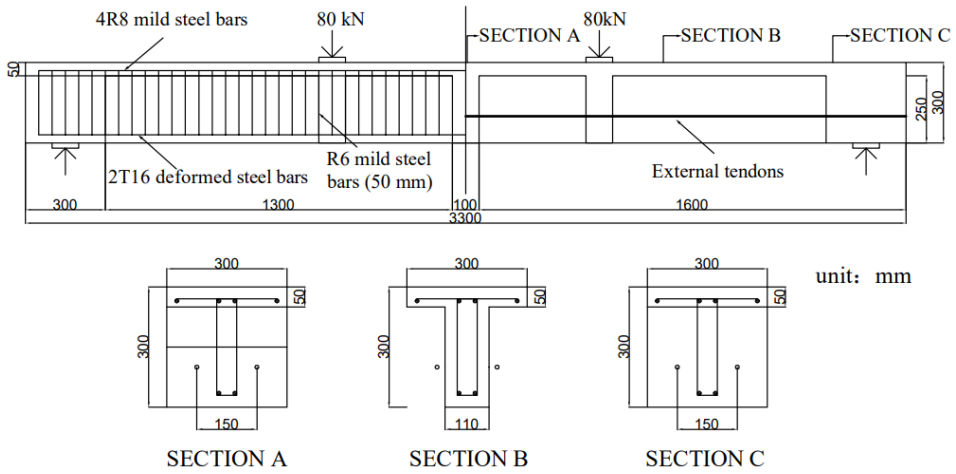

Fig. 1 The reinforcement drawing and section dimension of T-beam [14]

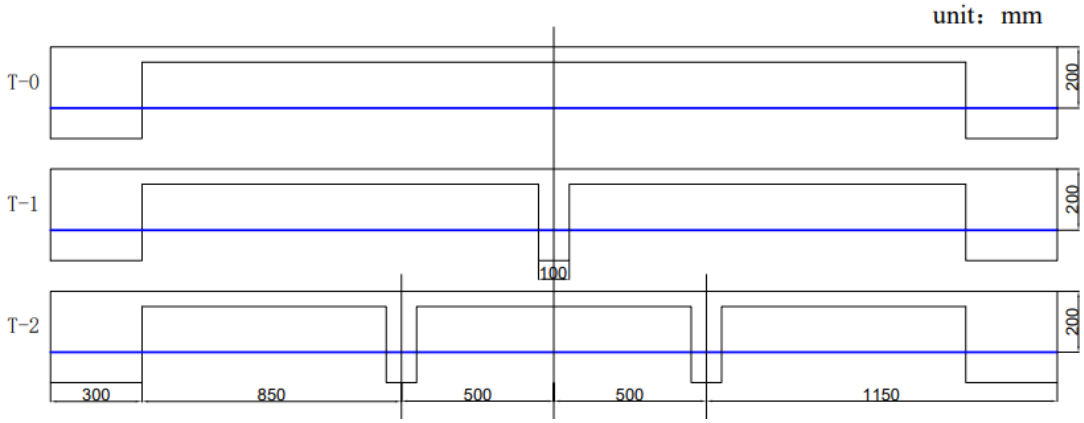

Fig. 2 The external tendon configuration of T-beam [14]

The lower reinforcement consisted of two deformed steel rebars (2T16), each with a diameter of 16 mm, while the upper reinforcement consisted of four mild steel rebars (4R8), each with a diameter of 8 mm. For the concrete, the water-cement ratio was 0.55 and the target cylindrical compressive strength of the concrete was 30 MPa at 28 days. The tendon had an equivalent diameter of 9.5 mm, an average tensile strength f_{pu} of 1900 MPa, and an elastic modulus E_{ps} of 193 GPa for three T-beams (T-0, T-1, and T-2). As shown in Table 1, the tendon arrangement and effective prestress of test beams with straight external tendons under third-point loading are as follows. The stirrup was composed of mild steel rebars with a diameter of 6 mm and a spacing of 50 mm, and the concrete cover was 30 mm thick vertically and 25 mm thick transversely. The material parameters of the specimens are given in Table 2 below. The Poisson's ratio is set at 0.3 for the steel rebars and at 0.2 for concrete.

Table1. Tendon configuration and effective prestress of test beams [14]

Beam	No. of deviator	Effective depth d_p (mm)	Effective prestress f_{pe} (MPa)	Tendon diameters d (mm)
T-0	0 (——)	200	1297	9.5
T-1	1 (Midspan)	200	1197	9.5
T-2	2 (1/3-span)	200	1182	9.5

Table2. The material parameters of the test specimens [14]

Beam	Steel rebars						External tendons				Concrete
	A_s (mm^2)	f_y (MPa)	E_s (GPa)	A'_s (mm^2)	f'_y (MPa)	E'_s (GPa)	A_p (mm^2)	E_f (GPa)	f_{pu} (MPa)	f_{pe} (MPa)	f_{ck} (MPa)
T-0	402	530	210	201	338	180	141.7	193	1900	1297	34.6
T-1	402	530	210	201	338	180	141.7	193	1900	1197	34.2
T-2	402	530	210	201	338	180	141.7	193	1900	1182	28.7

Note: A_s, f_y and E_s = area, yield strength, and elastic modulus of deformed steel rebars, respectively; A'_s, f'_y and E'_s = area, yield strength, and elastic modulus of mild steel rebars, respectively; A_p = tendon area; E_f and f_{pu} = elastic modulus and tensile strength of external tendons, respectively; f_{pe} = effective prestress.

2.2 Scheme of FEM

ABAQUS finite element software is frequently employed in scientific research for its powerful non-linear analytical capabilities. There are only a few correlated numerical analyses of prestressed T-beams post-tensioned with external tendons that have been reported in the open literature [13]. This study This study effectively establishes a 3D FEM using Abaqus/CAE for T-beams with external tendons, which is verified by previous literatures [14].

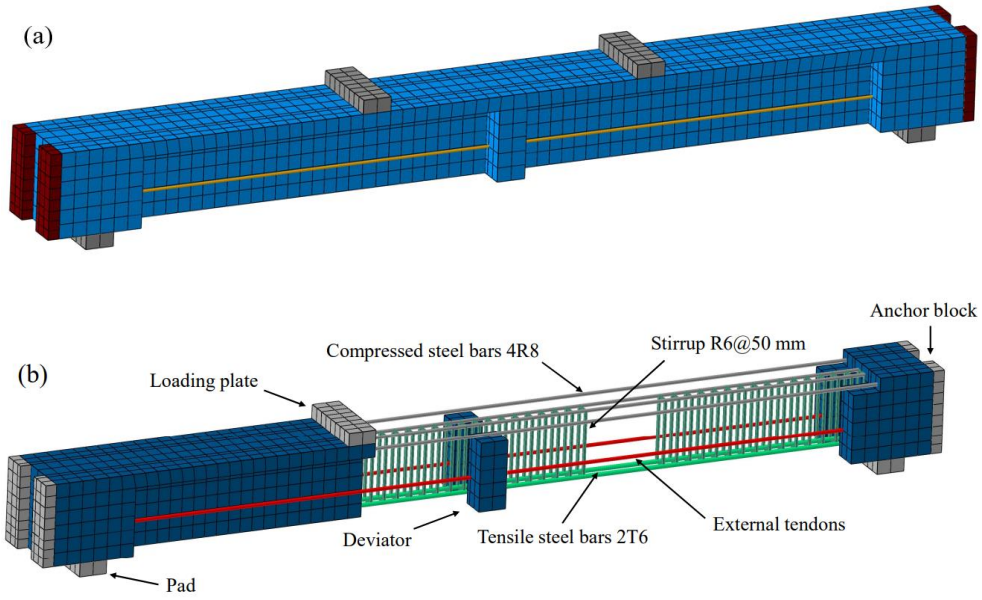

Fig. 3 3-D finite element model of T-1 beam with external tendons: (a) mesh and (b) configuration

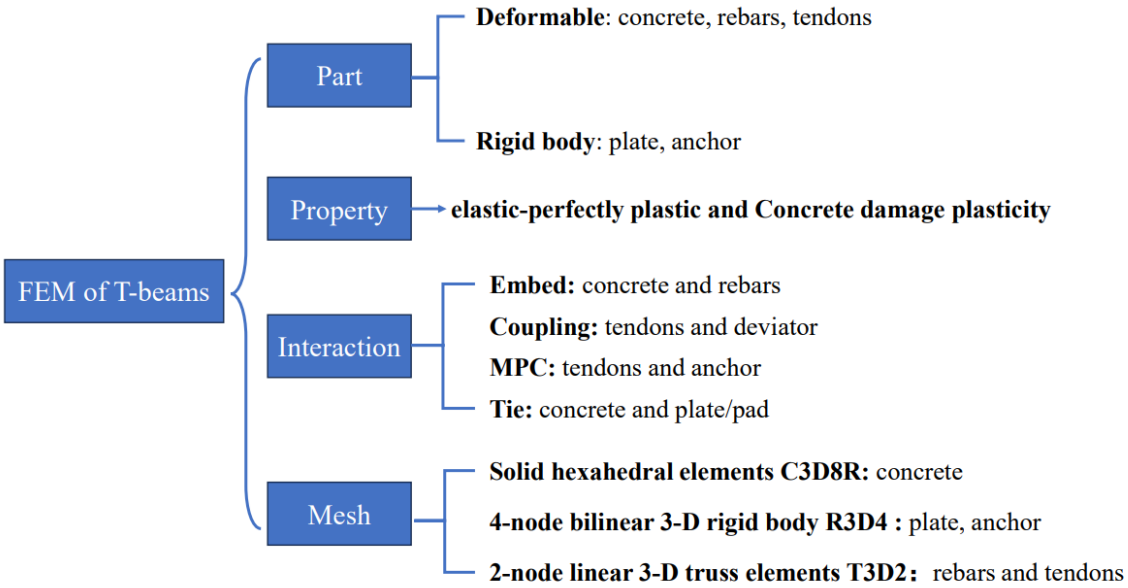

Fig. 4 The module setting of FEM in ABAQUS

This study solely displays the mesh and configuration of the revised ABAQUS FEM of T-1, as shown in Fig. 3. The module setting of FEM in ABAQUS is shown in Fig. 4. Solid hexahedral elements C3D8R were used to model the concrete elements, whereas 2-node linear 3D truss elements T3D2 were used to model the steel rebars and tendons, and 4-node bilinear 3D rigid bodies R3D4 were used to model the plate and pad. The difference between the temperature in initial step and the required temperature in next step [15] can be described as follows:

$$\Delta T_t = \frac{f_{pe}}{E_f \lambda} \quad (1)$$

where f_{pe} is the effective prestress of the external tendons; E_f is the elastic modulus of tendons; and λ is the thermal expansion coefficient. (For this study, E_f = 193 GPa, λ = 1.2×10^ (-5)/℃)

The concrete beam was meshed with a 45 mm mesh size, with a 20 mm mesh size in the critical region, where concrete and external tendons interact. Other components included an 80 mm mesh size for reinforcing bars and a 40 mm mesh size for steel plates and pads. Furthermore, it is assumed that the steel rebars and concrete were in a perfectly bonded state using the embedded region constraint. In addition, the unbonded tendons were coupled with concrete to constrain the degrees of freedom along the height and width of the beam, permitting them to slide along the length of the concrete beam, which can only simulate straight tendons, whereas for curved external tendons, rigid springs are used [16]. Using an ideal linear–elastic law and the concrete damage plastic model, the code for design of concrete structures GB50010-2010 [17] defines the properties of the steel bars and concrete.

3. VERIFICATION AND ANALYSIS OF FEM

3.1 FEM Verification

Using the ABAQUS FEM [18], the bending behavior of a self-compacting concrete T-beam with external tendons was accurately simulated. Fig. 5 depicts the damage cloud map of the T-2 beam caused by the creation and evolution of micro-defects during stress. In ABAQUS, concrete failure is defined by a damage coefficient ranging from 0 to 1, where 0 represents the unloaded condition and 1 represents total damage. The damage coefficient is 0.89 when the structure enters the ultimate condition in this study, although it is usually 0.9 when the concrete unit leaves service. Fig. 5 is the damage coefficient nephogram of the component at the ultimate state.

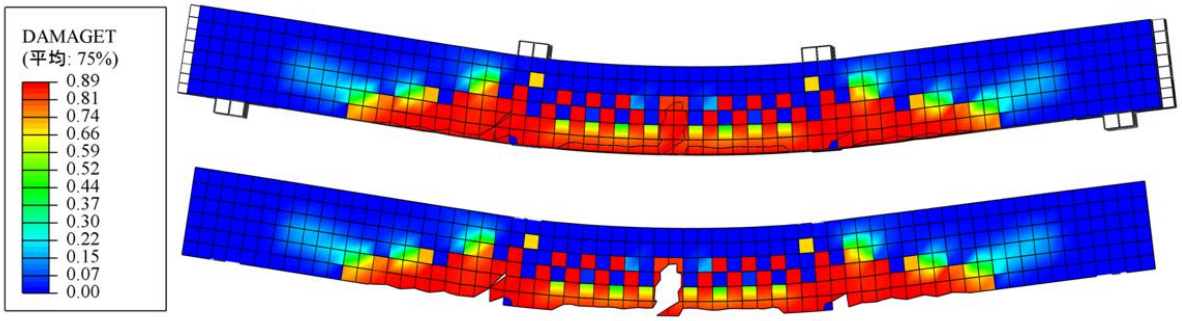

Fig. 5 Damage coefficient cloud diagram of T-2 beam

Numerical simulations based on ABAQUS finite element software were carried out for T-beams (T-0, T-1 and T-2) and the simulation results were compared with the load-deflection curves of the specimens [14] as shown in Fig. 6, where the solid lines are the experimental values and the dashed lines are the simulated values. When there was

no concrete cracking, the test results and the FEM results of the T-beams were virtually identical. After the fractures had stabilized (second stage), the deflection increased linearly with the applied loading. In the second step, the T-beam load-deflection curves at midspan were slightly lower than the simulated values, but they followed the same trend. This might be as a result of the strength of the selected concrete constitutive model being lower than the measured strength of the concrete. When flexural cracking occurred at around 25% of the ultimate load, all of the T-beams exhibited identical behavior, with a drop in beam stiffness. Table 3 compares the ultimate deflection and loading of the proposed 3D model with the experimental results for T- beams. By contrasting the predicted load-deflection behavior with test findings of externally prestressed beam published in the literature [14], the validity of the FEM is proven.

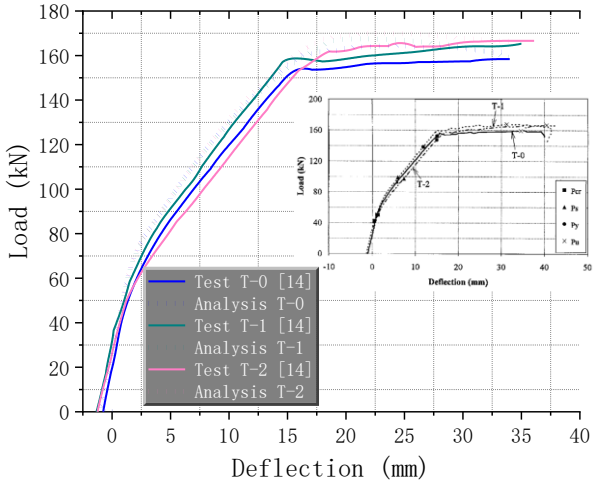

Fig. 6 Verification with experimental results: load versus midspan deflection.

Table3. Comparison of ultimate deflection and load obtained by the test and numerical analysis

Beam	Ultimate deflection Δ_u (mm)			Ultimate load F (kN)		
	Test	Numerical	Error (%)	Test	Numerical	Error (%)
T-0	36.52	34.32	-6.02	158.60	164.35	3.63
T-1	36.10	34.12	-5.48	164.51	167.49	1.81
T-2	36.93	34.69	-6.07	166.27	169.96	2.22

3.2 FEM Analysis

For the externally prestressed concrete beams, the tendons work together with the concrete through end anchors and deviators. The location of the deviators and anchors relative to the concrete section is invariable, therefore tendon eccentricity, except for the tendon fixed at anchors and deviators, will change and produce second-order effects. A more effective way of eliminating second-order effects is to allocate a certain number of deviators (especially at the maximum deflection), which can effectively improve the mechanical behaviors of externally prestressed structures [19]. The study is

to investigate the load-deflection behavior of T-2 and T-1 (with 2 deviators and 1 deviator) beams using concrete grade (C30, C40 and C50) and types of rebars (steel, CFRP and GFRP) as investigated variables. The material properties of the rebars and concrete are given in Tables 4 and Tables 5, respectively.

Table 4. Mechanical properties of rebars

Rebars	Tensile strength (MPa)	Yield strength (MPa)	Elastic modulus (GPa)
T16	530	530	200
R8	338	338	180
CFRP	1620	-	117
GFRP	750	-	50

Table 5. Mechanical properties of concrete

Concrete	Elastic modulus E_c (GPa)	Compressive strength f_c (MPa)	Tensile strength f_t (MPa)	Axial compressive strength f_{ce} (MPa)
C30	30.8	29.0	2.5	17.4
C40	33.3	37.8	2.9	22.7
C50	34.4	43.1	3.1	25.9

The load-deflection response of T-beams with three types of rebars and concrete grade is simulated and displayed in Fig. 7 under third-point stress up to failure. Fig. 7 clearly shows that the ultimate bearing capacity of the T-beam increases with increasing concrete grade for the same concrete cover thickness. For the same loading, the T-beam in the higher-grade concrete deflects less before the steel bars yield. The tendency for stiffness degradation increases significantly after reinforcement yielding in T-2 beam, which increases as the concrete grade decreases. The results also show that a higher concrete grade leads to a greater flexural capacity of the beams.

Before yielding, the steel-reinforced beams exhibit a response which is similar to the FRP-reinforced beams. Flexural stiffness in beams is significantly reduced after yielding of steel rebars. Due to little stress increments in rebars during the uncracking phase, the impact of rebars on reaction characteristics is negligible, which explains in part the reason. After cracking, the reactions of beams with FRP and steel rebars differ because the rebar contribution becomes increasingly relevant. The flexural stiffness decrease caused by cracking is significantly dependent on the rebar modulus of elasticity, i.e., the greater the elastic modulus of the rebar, the less the drop in member stiffness. As a result, GFRP rebars display higher post-cracking deformation than CFRP or steel rebars at given loading. For beams with FRP rebars, post-cracking distortion grows linearly till failure. The flexural stiffness of the beam with steel rebars is dramatically decreased on steel yielding.

The findings reveal that, compared to beams with GFRP or steel rebars, those with CFRP rebars display superior cracking mode and higher ultimate stress. They also demonstrate that higher concrete grade enhances beam flexing.

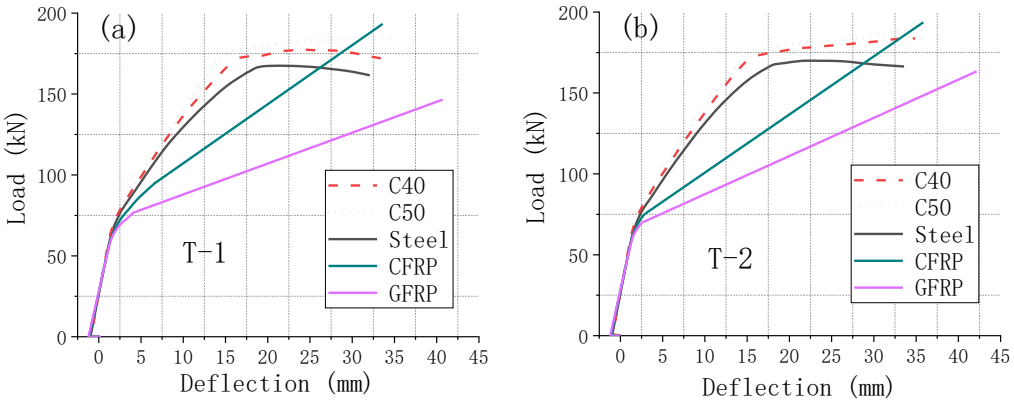

Fig. 7 Load-deflection response (a) T-1 beam; (b) T-2 beam

4. CONCLUSIONS

A refined 3D FEM was conducted on T-beams with external tendons, and the simulated results were compared with the experimental results, aimed at verifying the reliability of the model. Based on the investigation of the numerical model in the study, the following conclusions can be drawn:

- The temperature lowing method can effectively simulate the application process of external prestress in T-beams.
- The numerical model is capable of simulating the concrete damage process of T-beams with external tendons throughout the entire loading history, from prestressing to the ultimate limit state.
- The validity of the finite element model (FEM) is verified by comparing the predicted load-deflection behavior with the test results of externally prestressed T-beam which is available in the literature.
- The results indicate that the T-beams with CFRP rebars exhibit better crack mode and higher ultimate load than the T-beams with GFRP or steel rebars, and also show that a higher concrete grade leads to a greater flexural capacity of the beams.

ACKNOWLEDGMENT

The work has been supported by the Portuguese Foundation for Science and Technology under Grants No. 2022.04729.CEECIND, UIDB/00285/2020 and LA/P/0112/2020.

REFERENCES

[1] Fuhaid A F A, Niaz A. Carbonation and corrosion problems in reinforced concrete structures. Buildings, 2022, 12(5): 586.

[2] Du M, Wang D, Wang X, et al. Numerical simulation of reinforcement design and bearing capacity for external prestressing deviator based on strut-and-tie model. 2022 International Conference on Cloud Computing, Big Data and Internet of Things (3CBIT). IEEE, 2022: 213-218.
[3] Qi J, Ma Z J, Wang J, et al. Post-cracking shear behavior of concrete beams strengthened with externally prestressed tendons. Structures. Elsevier, 2020, 23: 214-224.
[4] Tan K H, Tjandra R A. Strengthening of RC continuous beams by external prestressing. Journal of Structural Engineering, 2007, 133(2): 195-204.
[5] Balafas I, Burgoyne C J. Economic design of beams with FRP rebar or prestress. Magazine of Concrete Research, 2012, 64(10): 885-898.
[6] ACI committee 440. Guide for the design and construction of structural concrete reinforced with FRP bars. ACI 440.1R-15, American Concrete Institute, Farmington Hills, MI; 2015.
[7] Abdallah M, Al Mahmoud F, Khelil A, et al. Assessment of the flexural behavior of continuous RC beams strengthened with NSM-FRP bars, experimental and analytical study. Composite Structures, 2020, 242: 112127.
[8] Xue W, Tan Y, Peng F. Experimental study on damaged prestressed concrete beams using external post-tensioned tendons. ACI Structural Journal, 2020, 117(1): 159-168.
[9] Du X, Wang Z, Liu J. Flexural capacity of concrete beams prestressed with carbon fiber reinforced polymer (CFRP) tendons. Advanced Materials Research. Trans Tech Publications Ltd, 2011, 168: 1353-1362.
[10] Park S Y, Hong S R, Kim C H. Fatigue behavior of reinforced concrete beams externally strengthened using FRP tendons. Journal of The Korean Society of Civil Engineer, 2008, 28(6): 809-817.
[11] Elrefai A, West J, Soudki K. Fatigue of reinforced concrete beams strengthened with externally post-tensioned CFRP tendons. Construction and Building Materials, 2012, 29: 246-256.
[12] Lin S C, Song J, Gao S, et al. Numerical simulation and field test studies on mechanical behavior of steel plate girder strengthened by external prestressed tendon. Structures. Elsevier, 2021, 33: 3188-3201.
[13] Tran D T, Pham T M, Hao H, et al. Numerical study on bending response of precast segmental concrete beams externally prestressed with FRP tendons. Engineering Structures, 2021, 241: 112423.
[14] Tan K H, Ng C K. Effects of deviators and tendon configuration on behavior of externally prestressed beams. ACI Structural Journal, 1997, 94(1): 13-22.
[15] Xiao X, Gu X, Zhang X. Combination of thermoacoustic heat dissipation with oscillating convection: A novel cooling method. International Journal of Heat and Mass Transfer, 2020, 160: 120177.
[16] Ozkul O.A new methodology for the analysis of concrete beams prestressed with unbonded tendons. Rutgers The State University of New Jersey,2007.
[17] MOHURD-China, AQSIQ-China. GB 50010-2010 (Modified in 2015) Code for design of concrete structures. (2015).
[18] Guo J, Qi B, Geng W, et al. Finite element modeling method and analysis of self-compacting concrete prestressed T-beam. IOP Conference Series: Earth and Environmental Science. IOP Publishing, 2021, 719(2): 022031.

[19] Lou T, Xiang Y. Numerical analysis of second-order effects of externally prestressed concrete beams. Structural Engineering and Mechanics, 2010, 35(5): 631-643.